NANO LETTERS

Letter

pubs.acs.org/NanoLett

MoO_{3-x} Nanowire Arrays As Stable and High-Capacity Anodes for Lithium Ion Batteries

Praveen Meduri,[†,∥] Ezra Clark,[†] Jeong H. Kim,[‡] Ethirajulu Dayalan,[⊥] Gamini U. Sumanasekera,[§] and Mahendra K. Sunkara*[,†]

[†]Department of Chemical Engineering, [‡]Conn Center for Renewable Energy Research, and [§]Department of Physics, University of Louisville, Louisville, Kentucky 40292, United States

[⊥]The ENSER Corporation, Pinellas Park, Florida 33781, United States

Supporting Information

ABSTRACT: In this study, vertical nanowire arrays of MoO_{3-x} grown on metallic substrates with diameters of ~90 nm show high-capacity retention of ~630 $mAhg^{-1}$ for up to 20 cycles at 50 mAg^{-1} current density. Particularly, they exhibit a capacity retention of ~500 $mAhg^{-1}$ in the voltage window of 0.7−0.1 V, much higher than the theoretical capacity of graphite. In addition, 10 nm Si-coated MoO_{3-x} nanowire arrays have shown a capacity retention of ~780 $mAhg^{-1}$, indicating that hybrid materials are the next generation materials for lithium ion batteries.

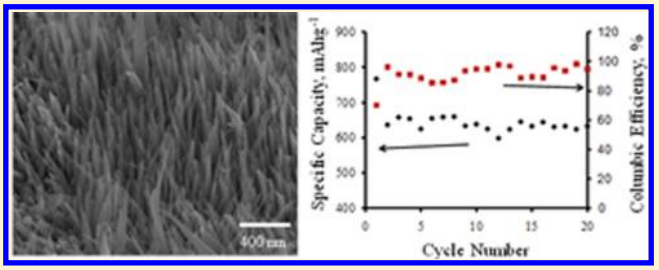

KEYWORDS: *Molybdenum oxide, anode, lithium ion battery, hybrid architecture, silicon*

Lithium ion batteries have gained tremendous interest for portable devices because of their superior energy capacity, long shelf life, and longer lifespan.[1] Safe, nontoxic, and high rate capable electrode materials present significant interest for use in hybrid electric vehicles.[2] The most widely used graphite anode has a theoretical capacity of 372 $mAhg^{-1}$ at ~0.1 V with regard to Li/Li^+. In practical systems, the extractable capacity of graphite anodes is much lower. Other forms of carbon, including carbon nanosprings[3] and carbon microtubes,[4] have shown to yield higher capacities but still have significant problems at low potential operation (<0.1 V). Metal oxides are possible choices for anode materials but suffer from capacity fading with cycling due to enormous volume expansion during lithium intercalation/deintercalation and poor kinetics. Recently, cobalt oxide,[5] Sn/SnO_2 hybrid architectures[6,7] and iron oxide[8] have shown high-capacity retention with low-capacity fading.

MoO_3 is a well-known lithium insertion material.[9] Bulk MoO_3 powders have shown high initial capacity but exhibited significant capacity fading with cycling. Recently, chemical vapor deposited MoO_3 nanoparticles exhibited a capacity of 630 $mAhg^{-1}$ for up to 150 cycles when cycled between 3.5 and 0.005 V,[10] and ball-milled MoO_{3-x} samples have exhibited a high initial discharge capacity of 1100 $mAhg^{-1}$ with capacity degradation upon cycling (~620 $mAhg^{-1}$ after 35 cycles).[11] In addition, the capacity in these electrodes is obtained over a wide potential with no obvious voltage plateaus which hinders their use as a practical electrode material. Recently, one-dimensional MoO_3 nanowires have been studied as potential electrode materials.[12−14] One-dimensional nanowires can provide good conduction pathways for electronic conductivity along with shorter path (diameter) for lithium diffusion. In this study, single crystalline MoO_3 nanowire arrays have been synthesized directly on conducting substrates and evaluated for electrochemical and lithium intercalation properties. Lower lithium intercalation voltages and flat voltage plateau have been observed making them suitable for practical use.

MoO_{3-x} nanowires were synthesized in a hot-filament chemical vapor deposition reactor in which molybdenum filaments were resistively heated to 775 °C in 10 sccm of oxygen at a pressure of 1.1 Torr. Under these conditions, the oxygen flow over Mo filaments resulted in molybdenum oxide vapor. Stainless steel substrates were placed 1.5 cm apart from the hot filament. MoO_{3-x} NW arrays were also grown on various other substrates, including copper, platinum mesh, quartz, and fluorinated tin oxide coated quartz. The synthesis was carried out for a duration of 30 min. Nanowire arrays were characterized for their morphology and crystal structure using scanning electron microscopy (SEM) (FEI Nova 600), X-ray diffraction (XRD) (Bruker D8 Discover, Cu Kα radiation), and Raman spectroscopy (in-Via Renishaw micro-Raman system with a cooled CCD detector) with a HeNe laser (632.8 nm) as an excitation source.

The as synthesized nanowires on conducting substrates were used as electrodes for electrochemical measurements. A three electrode cell consisting of a working electrode (nanowire

Received: October 16, 2011
Revised: February 3, 2012
Published: March 20, 2012

sample) and lithium as reference and the auxiliary electrode was employed. The electrolyte is a 1 M lithium hexaflourophosphate ($LiPF_6$) mixed in 1:1 volume ratio of ethylene carbonate (EC) and diethyl carbonate (DEC). The cell assembly and testing was carried out in a glovebox filled with argon using an eDAQ potentiostat and e-corder for all the electrochemical measurements.

Figure 1a shows that nanowire arrays with an average diameter of ~90 nm. The XRD spectrum presented in Figure1b

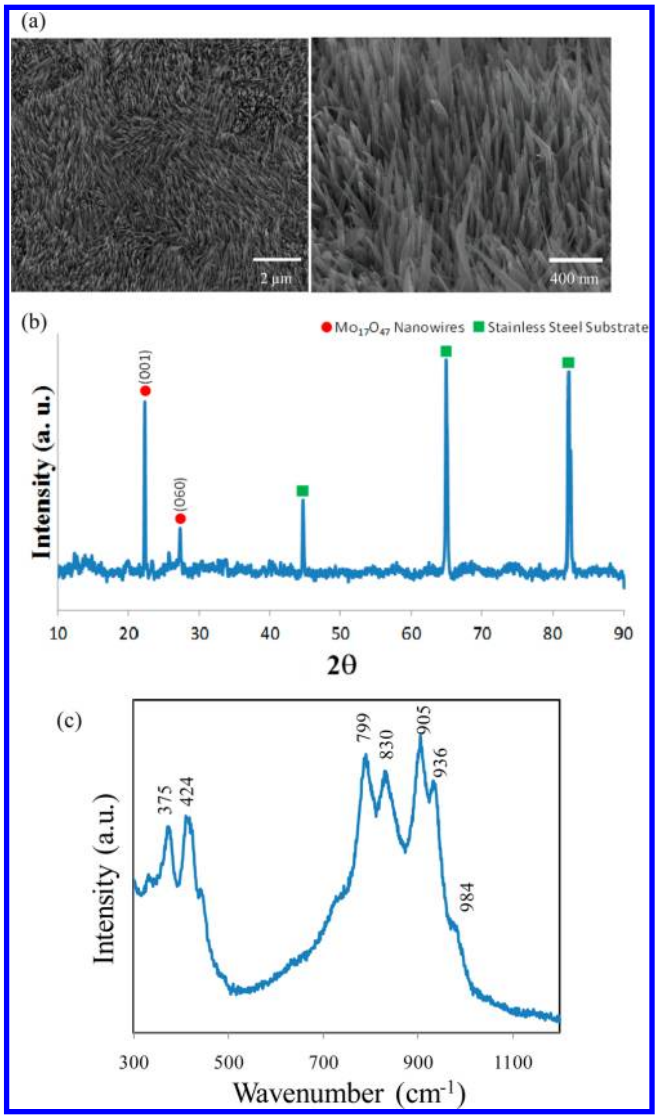

Figure 1. Characterization of as synthesized $Mo_{17}O_{47}$ nanowires. (a) SEM images showing the array architecture. (b) XRD spectrum corresponding to phase $M_{17}O_{47}$. (c) Raman spectrum indicating various Mo−O interactions.

indicates an oxygen deficient $Mo_{17}O_{47}$ phase.[15] The peak at 22.25° corresponds to the (001) plane of the orthorhombic $Mo_{17}O_{47}$ phase (JCPDS #01-071-0566). Three peaks beyond 40° were matched to the stainless steel substrate, and several small peaks in the 10−30° range correspond to the MoO_3 orthorhombic phase (JCPDS #01-089-5108). The presence of MoO_3 phase is likely due to sample's exposure to atmosphere. In many cases, the transition was visually observed with samples gradually changing colors upon prolonged exposure to air. Oxygen deficiency renders the dark-blue color to the resulting films. Raman spectrum for these arrays is shown in Figure 1c. The peaks at higher wavenumbers (905 and 984), 830 and 799 cm^{-1} correspond to Mo−O, Mo−O_2, and Mo−O_3 vibrations, respectively.[15] The presence of multiple peaks indicates complex interactions of Mo and O atoms, further indicating that the nanowire arrays are oxygen deficient.

Three electrode configuration cells with MoO_{3-x} nanowire anode materials were cycled between 100 mV and 3.5 V. The data in Figure 2a show that the specific capacity retention of the nanowires is ~630 $mAhg^{-1}$ for up to 20 cycles. The initial discharge capacity is ~770 $mAhg^{-1}$ at a current density of 25 mAg^{-1}, corresponding to 4.1 Li^+ ions per MoO_{3-x}. The second cycle discharge capacity is ~635 $mAhg^{-1}$, which remains constant until 20 cycles, at a current density of 50 mAg^{-1}. MoO_{3-x} electrodes in the present study are cycled to only 100 mV to prevent lithium plating but comes at the expense of capacity. The first cycle irreversible capacity loss is 176 $mAhg^{-1}$ corresponding to a columbic efficiency of 70%, which usually is quite low in transition metal oxide systems. The columbic efficiency as indicated in Figure 2a is over 90% for the subsequent cycles. Even though the tests were performed for only 20 cycles, the data clearly shows that the capacity retention of MoO_{3-x} nanowires is significant and the discharge potential, 0.7 V vs Li/Li^+, is low enough for practical applications. The lithiation in MoO_3 is believed to take place in two stages: Stage I occurs up to a potential of 1.5 V. During this stage, Li intercalates with MoO_3 as follows:[16]

$$MoO_3 + xLi^+ + xe^- \rightarrow Li_xMoO_3 \quad (1)$$

The lithium content in this solid solution ranges between 1 and 1.5, up to a potential of 1.5 V. The high lithium content is accommodated in the interlayer spacing between octahedral Mo−O layers and intralayers. Most of the Li ions intercalated at these potentials can subsequently be extracted from the material leading to reversibility of the reaction.

Lithium ion intercalation during stage II corresponds to potentials below 0.7 V and occurs by the following mechanism:[17]

$$Li_xMoO_3 + yLi^+ + ye^- \rightarrow Mo + 3Li_2O \quad (2)$$

In the lower voltage range, lithium reacts with the solid solution to consequently form metal and Li_2O. However, Li_2O is primarily irreversible, but the presence of nanoscale metal particles leads to the reversibility of Li_2O, which has been reported earlier.[6,7] Discharge curves presented in Figure 2b indicate a curve which is continuous and smooth until 0.7 V followed by a plateau after repeated cycling, unlike the bulk material which does not show significant capacity in the low-voltage region. MoO_3 nanoparticles have been known to show similar two-stage behavior; however, the curves in that particular case are continuous and have a much lower capacity retention below 0.7 V. This reversibility of Li_2O is a primary reason for the observed columbic efficiencies >90% for MoO_{3-x} nanowires studied here.

The differential capacity curves shown in Figure 2c,d support the two stage mechanism. The first cycle differential capacity (DC) curve shows a small peak in the higher potential region above 1.5 V and multiple peaks in the lower potential region below 0.5 V. These peaks indicate the Li intercalation by a mechanism shown in eqs 1 and 2. DC curves for the next few cycles also indicate peaks above 1.5 V and below 0.5 V, further confirming the mechanism. These peaks appear until the tenth

dx.doi.org/10.1021/nl203649p | Nano Lett. 2012, 12, 1784−1788

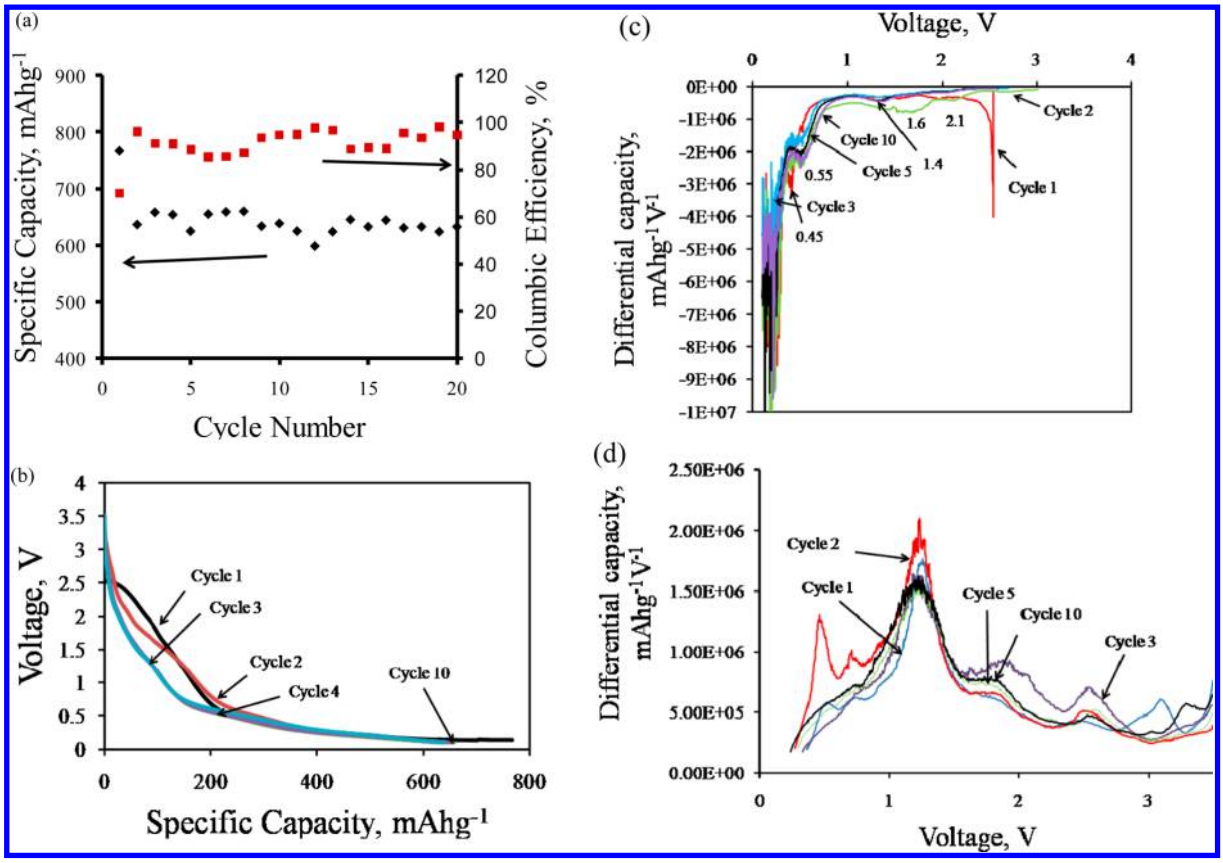

Figure 2. Electrochemical characteristics of MoO_{3-x} nanowires. (a) Specific capacity at current density of 50 mAg^{-1} (first cycle: 25 mAg^{-1}). Secondary axis is the columbic efficiency. (b) Discharge profiles until 10 cycles indicating plateau below 0.7 V. (c) DC curves during discharge indicating lithiation. (d) DC curves during charge indicating delithiation characteristics.

cycle, as indicated in Figure 2c, showing excellent reversibility of the electrode.[18] Figure 2d shows the DC curves for the charge cycle of MoO_{3-x} NW arrays. The charge cycles clearly indicate peaks around 0.5, 1.2, 1.8, and 2.6 V, indicating that the delithiation occurs in two stages. In addition, the peak occurrence suggests that MoO_{3-x} is formed reversibly with low loss in the capacity with cycling.

A complete reduction of MoO_3 requires six Li^+ ions per Mo. The first cycle capacity of ~770 $mAhg^{-1}$ corresponds to 4.1 Li^+ ions per one Mo atom, of which 1.1 Li^+ ions are intercalated as indicated in eq 1. The remaining three Li^+ ions intercalate with the solid solution by the mechanism indicated in eq 2. This indicates an incomplete conversion to Li_2O and Mo. Further cycles indicate capacities close to ~650 $mAhg^{-1}$ corresponding to 3.4 Li^+/Mo. However, the data over next few cycles show interesting behavior, i.e., the addition of lithium (eq 1) accounts for less than 100 $mAhg^{-1}$ that corresponds to only ~0.6 Li^+/Mo. The reaction shown in eq 2 accounts for ~500 $mAhg^{-1}$ capacity equivalent to 2.8 Li^+/Mo, indicating a good reversibility of this reaction. The data pertaining to capacity retention between 0.7 and 0.1 V are presented in Figure 3a, which makes the materials practically usable. See Figure S1, Supporting Information, for 20 cycle data. Nanowire arrays have shown capacity retentions of 632 and 590 $mAhg^{-1}$ at current densities of 50 mAg^{-1} and 100 mAg^{-1}, respectively (Figure 3b). It is to be noted that a capacity of 685 $mAhg^{-1}$ at 25 mAg^{-1} is obtained on switching from the high rate back to the low rate. These nanowire arrays can hence, be used as base materials to develop hybrid architectures with high-capacity materials. Si is particularly interesting as the intercalation potentials of Si and MoO_3 match well at ~0.7 V, making them ideal hybrid materials.

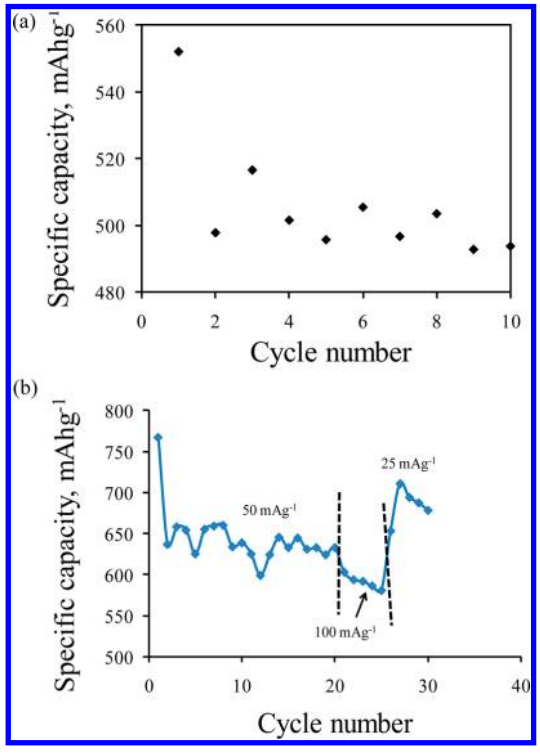

Figure 3. Practical applicability of MoO_{3-x} nanowire arrays. (a) High-capacity retention below 0.7 V. (b) Rate performance of the material.

dx.doi.org/10.1021/nl203649p | Nano Lett. 2012, 12, 1784–1788

In order to prove the hybrid architecture proposition, MoO_{3-x} nanowire arrays were coated with silicon. The transmission electron microscopy (TEM) image presented in Figure 4a shows a 10 nm Si deposition on the surface.

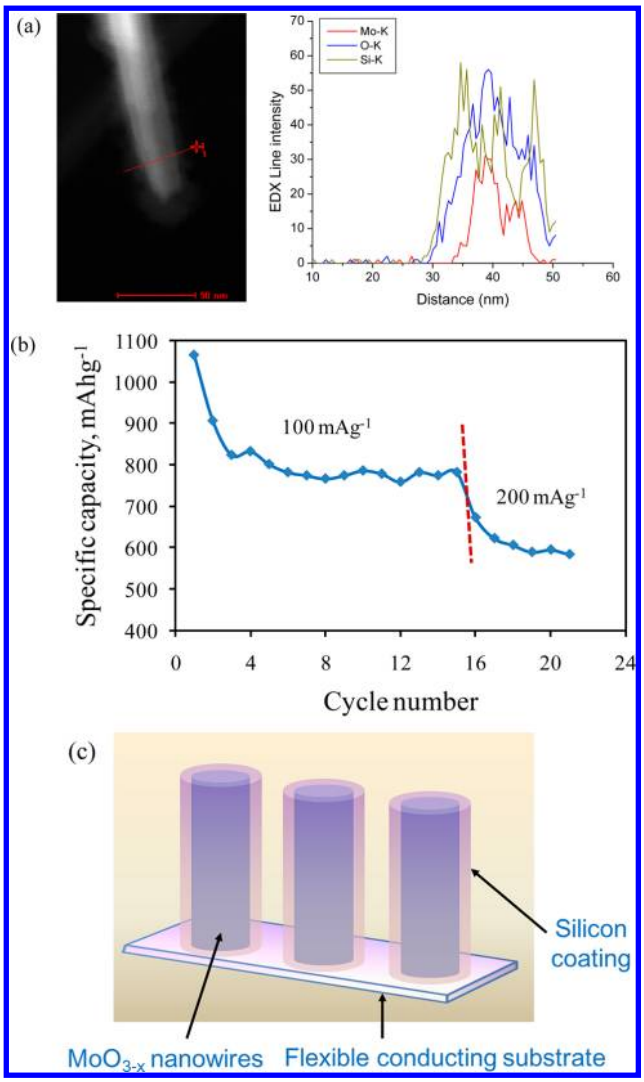

Figure 4. Si/MoO_{3-x} hybrid architectures. (a) Line scan in a TEM showing 10 nm silicon coating on MoO_{3-x} nanowires. (b) Hybrid materials with capacity of 780 and 580 $mAhg^{-1}$ at rates of 100 and 200 mAg^{-1}, respectively. (c) Schematic of MoO_{3-x} nanowire array covered with silicon for stable and high-capacity retention.

However, line scan of the image shows the presence of low amounts of oxygen in silicon. Figures S2 and S3, Supporting Information, show experimental schematic used and the SEM images of the silicon-coated MoO_{3-x} nanowire arrays, respectively. In theory, ~10% silicon is present in these samples (by weight) which corresponds to a theoretical capacity of ~1370 $mAhg^{-1}$ for the sample, compared to 1116 $mAhg^{-1}$ for pure MoO_{3-x} nanowire arrays. The specific capacity data in Figure 4b show that the hybrid material shows an initial capacity of 1065 $mAhg^{-1}$ with capacity retention of ~780 $mAhg^{-1}$ until 15 cycles at a current density of 100 mAg^{-1}. The rate performance presented in Figure 4b shows a stable performance of ~580 $mAhg^{-1}$ at 200 mAg^{-1}. The capacity of these may be significantly improved by thicker Si deposition. In a typical MoO_3 nanowire array sample, there is about $10^9/cm^2$ density of MoO_{3-x} nanowires, which leaves about 50% volume for including silicon to obtain a 50−50 mixture of Si and MoO_{3-x} hybrid material with a theoretical capacity of ~2650 $mAhg^{-1}$. A schematic illustrating the silicon coating on MoO_{3-x} nanowire array in Figure 4c with ample expansion volume should lead to ideal Si-based hybrid architectures for high capacity and high rate capability.

In this study, MoO_{3-x} nanowire arrays are shown to retain a capacity of ~630 $mAhg^{-1}$ for up to 20 cycles at a current density of 50 mAg^{-1}. These nanowire arrays undergo a two stage lithiation/delithiation mechanism which occurs above 1.5 V and below 0.7 V, leading to a retention of 3.4 Li ions per Mo. In addition, nanowire arrays show a good capacity retention of ~500 $mAhg^{-1}$ below 0.7 V, indicating viable practical applicability of the material. In addition, Si/MoO_{3-x} hybrid nanowires synthesized by the direct deposition of Si on MoO_{3-x} nanowire arrays have shown higher capacity retentions of ~780 $mAhg^{-1}$, paving ways for higher capacity stable anode materials.

■ ASSOCIATED CONTENT

Supporting Information

Figure S1 indicates the specific capacity of the MoO_{3-x} NWs in the lower potential range for 20 cycles. Figure S2 shows the reactor setup used for the silicon coating on the MoO_{3-x} nanowires. Figure S3 corresponds to the SEM image of pure MoO_{3-x} NW arrays and silicon-coated MoO_{3-x} nanowire array with the diameter scales. This material is available free of charge via the Internet at http://pubs.acs.org.

■ AUTHOR INFORMATION

Corresponding Author

*E-mail: mahendra@louisville.edu

Present Address

‖Pacific Northwest National Laboratory, Richland, WA 99352, United States.

Notes

The authors declare no competing financial interest.

■ ACKNOWLEDGMENTS

The authors gratefully acknowledge the financial support from the US Department of Energy (DE-FG02-05ER64071 and DE-FG02-07ER46375).

■ REFERENCES

(1) Scrosati, B. *Nature* **1995**, *373*, 557−558.
(2) Tarascon, J. M.; Armand, M. *Nature* **2001**, *414*, 359−367.
(3) Wu, X.-L.; Liu, Q.; Guo, Y.-G.; Song, W.-G. *Electrochem. Commun.* **2009**, *11*, 1468.
(4) Meduri, P.; Kim, J. H.; Benjamin, H. R.; Jasinksi, J.; Sumanasekera, G. U.; Sunkara, M. K. *J. Phys. Chem. C* **2010**, *114*, 10621.
(5) Li, Y.; Tan, B.; Wu, Y. J. *Nano Lett.* **2008**, *8*, 265.
(6) Meduri, P.; Pendyala, C.; Kumar, V.; Sumanasekera, G. U.; Sunkara, M. K. *Nano Lett.* **2009**, *9*, 612.
(7) Meduri, P.; Clark, E.; Dayalan, E.; Sumanasekera, G. U.; Sunkara, M. K. *Energy Environ. Sci.* **2011**, *4*, 1695.
(8) Taberna, P. L.; Mitra, S.; Poizot, P.; Simon, P.; Tarascon, J. −M. *Nat. Mater.* **2006**, *5*, 567.
(9) Whittingham, M . S. *J. Electrochem. Soc.* **1976**, *123*, 315.

(10) Lee, S.-H.; Kim, Y.-H.; Deshpande, R.; Parilla, P. A.; Whitney, E.; Gillaspie, D. T.; Jones, K. M.; Mahan, A. H.; Zhang, S.; Dillon, A. C. *Adv. Mater.* **2008**, *20*, 1.
(11) Jung, Y. S.; Lee, S.; Ahn, D.; Dillon, A. C.; Lee, S.-H. *J. Power Sources* **2009**, *188*, 286.
(12) Mai, L. Q.; Hu, B.; Chen, W.; Qi, Y. Y.; Lao, C. S.; Yang, R. S.; Dai, Y.; Wang, Z. L. *Adv. Mater.* **2007**, *19*, 3712.
(13) Chen, J. S.; Cheah, Y. L.; Madhavi, S.; Lou, X. W. *J. Phys. Chem. C* **2010**, *114*, 8675.
(14) Zhou, L.; Yang, L.; Yuan, P.; Zou, J.; Wu, Y.; Yu, C. *J. Phys. Chem. C* **2010**, *114*, 21868.
(15) Dieterle, M.; Mestl, G. *Phys. Chem. Chem. Phys.* **2002**, *4*, 822.
(16) Yu, A.; Kumagai, N.; Liu, Z. L.; Lee, J. Y. *Solid State Ionics* **1998**, *106*, 11.
(17) Dickens, P. G.; Reynolds, G. J. *Solid State Ionics* **1981**, *5*, 331.
(18) Mariotti, D.; Lindström, H.; Bose, A. C.; Ostrikov, K. *Nanotechnology* **2008**, *19*, 495302.